International Journal of Frontier Technology and Engineering (IJFTE)
Vol. 04 No. 1, 21 December 2025, pp. 1-11

Field-Oriented Regenerative Braking Control for Electric Vehicles

Zakiyah Amalia[1], Achsanul Khabib[2], Erni Yudaningtyas[3], Talifatim Machfuroh[1], Siti Duratun Nasiqiati Rosady[1], and Fica Aida Nadhifatul Aini[1]

[1]*Department of Mechanical Eng., State Polytechnic of Malang, Jl. Soekarno - Hatta 9, Malang-Indonesia*
[2]*Department of Electrical Eng., State Polytechnic of Malang, Jl. Soekarno - Hatta 9, Malang-Indonesia*
[3]*Department of Electrical Eng., University of Brawijaya, Jl. M.T. Haryono 167, Malang, Indonesia*

Corresponding Author: Achsanul Khabib, achsanul.khabib@polinema.ac.id

Received Date: 10-03-2025 Revised Date: 14-05-2025 Accepted Date: 07-12-2025

Abstract

Most electric vehicle designs use regenerative braking to convert energy losses during braking back into the battery. there have been studies with several approaches. Some research is on the evaluation and functionality test of the regenerative braking system, but the system remains to be improved and modified. The author proposes a braking mechanism that uses variable ADC (analog to digital converter) to control the intensity of braking. The braking system is used to slow down the speed of the vehicle or even stop a vehicle from running. The author proposes to combine mechanical braking and regenerative braking to optimize the braking system because if only a regenerative brake is used, the vehicle is not properly stopped. The regenerative brake system is used to convert the kinetic energy from the vehicle to the battery through a BLDC hub that is controlled by the converter. This converter can manage the intensity of the braking during deceleration. An integrated braking system for electric vehicles is proposed using the Field-Oriented Control (FOC) method to achieve optimization between braking performance and mechanical endurance. Unlike the conventional FOC algorithm , the braking system in this research inverses the direction of the magnetic field force of the BLDC stator coil from driving to braking. FOC braking provides better control during braking of electric vehicles and energy savings. The energy recovered from braking was 11.7% of the energy consumed during acceleration. The experiment was conducted on a road with real-time data recording to measure the energy recovered from the braking process, using a modified 250-watt BLDC motor. it can be concluded that the energy recovered from the braking was 11.7% of the energy consumed during acceleration.

Keywords : BLDC Hub, Regenerative braking, Field Oriented Control, Converter, Electric vehicles

1 Introduction

Most electric vehicle designs incorporate regenerative braking, which converts energy losses during braking back into the battery. Several studies have explored various approaches to this technology [1] [2]. Some research focuses on the evaluation and functional testing of regenerative brake systems [3], although there is still room for improvement and modification. The author proposes a braking mechanism that utilizes a variable Analog-to-Digital Converter (ADC) to control the braking intensity. This system is intended to slow down or stop a moving vehicle. Furthermore, the author suggests combining mechanical and regenerative braking to optimize overall performance, as relying solely on regenerative braking may not effectively bring the vehicle to a complete stop.

The regenerative braking system is an electric braking mechanism that decelerates the vehicle while recovering kinetic energy during braking. Unlike conventional braking systems, where energy is dissipated as heat,

regenerative braking converts this energy into electrical energy, which can be used to recharge the vehicle's battery, thereby extending its driving range. The key factors influencing the performance of regenerative braking include the rotational speed of the motion source, the input power to the generator, and the output power generated. These factors significantly impact the overall efficiency of the system. The block diagram of the regenerative braking system is shown in Figure 1. A regenerative braking system converts the kinetic energy of the vehicle into electrical energy, which is transferred to the battery through a BLDC hub motor controlled by a converter. This converter regulates the braking intensity during deceleration. The system's block diagram is illustrated in Figure 1.

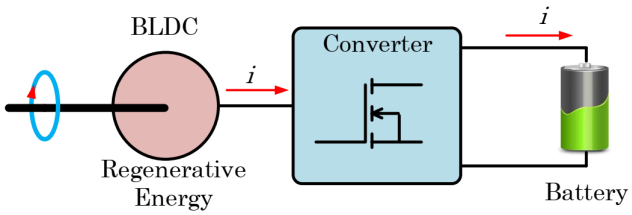

Figure 1: Block diagram of the braking system on a hub-type BLDC machine

In conventional braking systems, braking occurs when the brake lever is pulled or the pedal is pressed, causing the brake pads to attach to the wheel rotors. This process converts mechanical energy into heat energy, leading to inefficiencies. When applied to electric motorcycles, such braking systems become less effective. Therefore, regenerative braking systems are used in electric motorcycles to improve efficiency by recovering and storing energy during braking.

This study proposes an integrated braking system for electric vehicles using the Field-Oriented Control (FOC) method to optimize both braking performance and mechanical durability. Unlike conventional FOC algorithms [4] [5], the braking system in this research reverses the magnetic field force in the BLDC stator coil from driving to braking mode [6] [7] [8]. This braking mechanism, commonly used in heavy-duty systems, allows the vehicle to rapidly decelerate when inertia is high. In practice, the action of the brake causes the electric motor to generate torque in the opposite direction. When the BLDC motor receives a braking signal, the reverse rotor torque is produced by altering the current direction through the MOSFETs. This study provides a theoretical explanation of the regenerative braking system, supported by experimental validation.

2 BLDC HUB Model

The HUB-type BLDC motor is an out-runner BLDC, where the rotor consists of a permanent magnet and the stator is positioned at the center as a coil. This type of BLDC motor is commonly used in electric vehicles, particularly electric bikes, because of its ease of installation and the reduction in mechanical components that require maintenance or replacement. As a direct-drive motor, the HUB-type BLDC transfers power directly to the wheel without intermediate components. The cross-sectional view of the BLDC Hub is depicted in Figure 2. A BLDC motor can be described as three coils of wire arranged in a Y-configuration, each winding possessing its own resistance and inductance. In a BLDC motor, the inductance and resistance values are identical for each winding. The equivalent circuit model of the BLDC Hub motor is shown in Figure 3. Based on Figure 3, a BLDC hub machine can be identified using Kirchoff's law equation as follows:

$$\frac{d}{dt}\begin{bmatrix} i_u \\ i_v \\ i_w \end{bmatrix} = \frac{1}{L_s - M}\mathbf{I}_3 \left(\begin{bmatrix} V_{uQ} \\ V_{vQ} \\ V_{wQ} \end{bmatrix} - R_s \mathbf{I}_3 \begin{bmatrix} i_u \\ i_v \\ i_w \end{bmatrix} - \begin{bmatrix} e_u \\ e_v \\ e_w \end{bmatrix} \right) \tag{1}$$

where v_u, v_v, v_w are the three-phase voltages of the BLDC motor, i_u, i_v, i_w are the three-phase currents, R_s is the internal resistance of the BLDC motor, $\mathbf{I}_3$ is the 3×3, L_s is the self-inductance, M is the mutual inductance and e_u, e_v, e_w are the back electromotive forces.

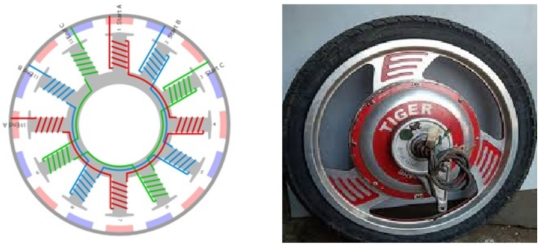

(a) (b)

Figure 2: The structure of the Hub type BLDC. (a) Stator and Rotor view (b) Photo view of BLDC hub

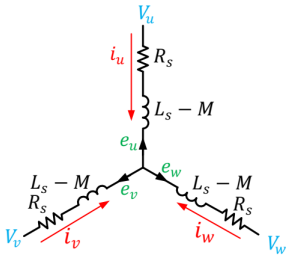

Figure 3: Equivalent circuit of BLDC Hub.

3 Control Strategy

3.1 System Architecture

Field-Oriented Control (FOC) is a type of vector control method used to regulate torque and flux in the d and q coordinates of a BLDC motor. This control technique involves determining the angular difference between the magnetic field of the rotor and the magnetic field of the stator. If the angle between these two fields deviates from 90 degrees, a phase offset occurs between the back-EMF and the current, leading to reduced efficiency. To address this issue, the FOC controller adjusts the control logic to maintain a 90-degree angle between the fields, ensuring that the torque generated by the BLDC motor is maximized [9], [10], [11], [12]. The main advantages of the FOC controller include reducing motor vibrations caused by PWM switching and improving motor efficiency by optimizing power consumption [10]. If the angle of the magnetic field of the rotor can be detected accurately, it becomes possible to generate a rotating magnetic field that maintains a 90^o separation from the magnetic field of the rotor. This 90^o angle ensures that torque production is maximized.

Field-Oriented Control (FOC) achieves this by operating the motor at full torque while continuously monitoring the angular position of the rotor [13], [14]. The system then adjusts the three-phase voltage to ensure that the back EMF on the armature remains 90 degrees apart from the rotor flux [15] [16]. This method is straightforward: by measuring the angular position of the rotor and adding 90^o, the three-phase voltage can be calculated to maintain the required 90^o phase difference [17].

$$P = S + I + Rv_u = V_m \sin\theta \tag{2}$$

$$v_v = V_m \sin(\theta - 120^\circ) \tag{3}$$

$$v_w = V_m \sin(\theta - 240^\circ) \tag{4}$$

The Field-Oriented Control (FOC) algorithm generates a three-phase voltage vector to regulate the three-phase stator current. By transforming physical currents into a rotating reference frame, the components of torque and flux become invariant in time [18], [19]. This transformation allows for the use of conventional control techniques, such as Proportional-Integral (PI) controllers, similar to those used in DC motors.

In a brushed DC motor, the stator flux and the rotor flux are maintained at a 90-degree angle to each other, resulting in maximum torque production. The Field-Oriented Control (FOC) technique similarly converts the motor current into a two-axis vector, analogous to the approach used with DC motors [20], [21]. The process begins by measuring the three-phase motor currents, as given in Fugre 4. However, in practice, measuring only two of the three currents is sufficient to determine the third current, which reduces hardware costs by requiring only two current sensors [22].

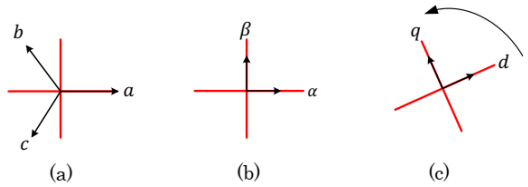

Figure 4: The coordinate system of FOC. (a) 3-axis stator reference, (b) 2-axis stator reference, and (c) 2-axis rotating reference.

The Field-Oriented Control (FOC) algorithm is illustrated in a block diagram that includes coordinate transformation, *PI* control iteration, back transformation, and PWM generation. This diagram outlines the functions necessary to implement the FOC control. The error signals from the i_d and i_q components, along with reference values for i_d, are used to manage the magnetization flux of the rotor. To achieve maximum torque, the flux vector must remain aligned with the magnetic poles of the rotor, which is ensured by maintaining a zero flux reference. Here, i_d and i_q represent the flux and torque components, respectively. The reference value for i_q controls the torque output of the motor [23]. The PI controller outputs V_d and V_q, which are the voltage vectors applied to the BLDC motor. The new angle of coordinate transformation is computed based on the motor speed, the time constant of the rotor voltage, and the values i_d and i_q [24]. The proposed FOC algorithm is illustrated in Figure 5.

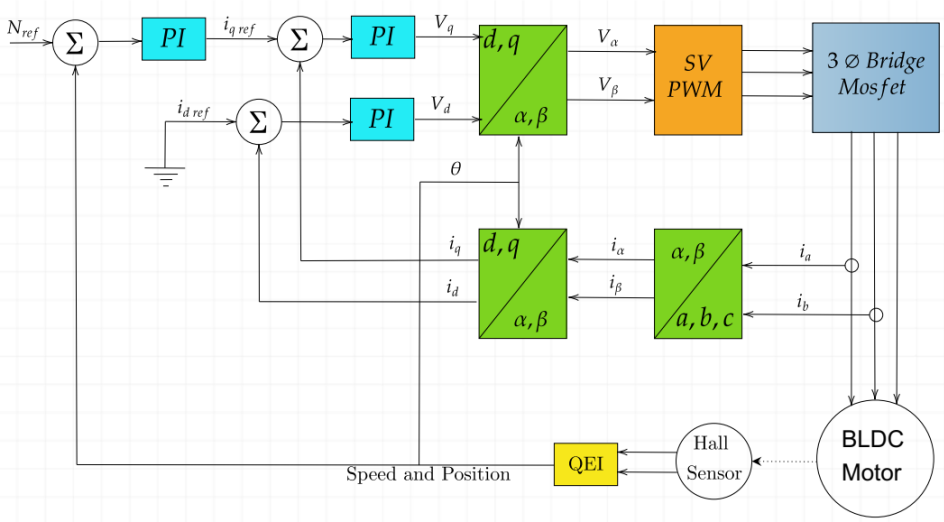

Figure 5: The proposed algorithm

Field-Oriented Control (FOC) operates by using the updated angle to determine the next voltage vector

required to generate the necessary torque to maintain the rotor motion. The output values V_d and V_q of the PI controller are converted back to the stationary reference frame using this new angle, resulting in the quadrature voltage components v_α and v_β. These values v_α and v_β are then transformed into three-phase voltages V_a, V_b and V_c. The three-phase voltage values are used to compute the PWM cycle, which generates the desired voltage vector. The transformation angle θ and the motor speed are obtained from the hall sensor mounted on the motor shaft.

3.2 Power Driver Design

The inverter topology is illustrated in Figure 6. In this diagram, V_{Batt} represents the voltage source with an associated capacitor C. The topology includes six MOSFETs with body diodes. For a clearer understanding of how Space Vector Pulse Width Modulation (SVPWM) operates, the two-bridge MOSFET configuration can be simplified to show only the switches that indicate whether the top or bottom MOSFET is closed. This simplification is valid because, in each leg of the bridge, only one MOSFET is closed at a time, and each leg must be closed to allow the three-phase current to flow. A simplified diagram is shown in Figure 6. The SVPWM method utilizes six basic voltage vectors that correspond to different voltage states applied to the motor terminals. The eight SVPWM states transition as follows [25] [26]: V_0 (000) $\rightarrow$ V_1 (001) $\rightarrow$ V_2 (011) $\rightarrow$ V_3 (010) $\rightarrow$ V_4 (110) $\rightarrow$ V_5 (100) $\rightarrow$ V_6 (101) $\rightarrow$ V_7 (111). These states represent combinations of voltage variations of 0, $-V_s$, and V_s applied to the voltages V_{uv}, V_{vw}, and V_{wu}.

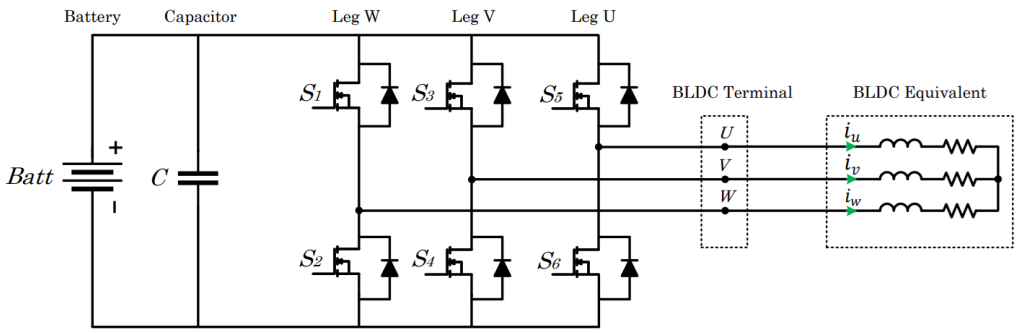

Figure 6: Power Topology on the BLDC controller

To determine the rotor reference position in the d–q coordinate system, the method described by [12] can be used. This method involves calculating the position of the rotor using the techniques outlined in their study.

$$\frac{dI_d}{dt} = -\frac{R_s}{L_d} I_d + \omega_r \frac{L_q}{L_d} I_q + V_d \tag{5}$$

$$\frac{dI_q}{dt} = -\frac{R_s}{L_q} I_q - \omega_r \frac{L_d}{L_q} I_d - \frac{1}{L_q} \phi \omega_r + V_q \tag{6}$$

so that

$$\varphi_d = L_d I_d + \varphi_f, \quad \varphi_q = L_q I_q \tag{7}$$

where L_q and L_d are inductances on the d-axis and the q-axis, While I_d and I_q are stator currents, P is the number of poles, φ_f is mutual flux produce magnet, R_s is the stator resistance, V_d and V_q is the voltage d and q-axis, while L_s is self-inductance. The electromagnetic torque is written by the equation:

$$T_e = \frac{3}{2} P \left[(L_d - L_q) I_d I_q + I_q \varphi_f \right] \tag{8}$$

in this equation if $I_d = 0$, then the flux φ_d on the d-axis is constant. since φ_f is constant, the electromagnetic torque T_m is determined by the equation:

$$T_m = \frac{3}{2} P \varphi_f I_d \tag{9}$$

The current vector is generated on the FOC-axis, and the rotor flux is generated only on the q-axis. This setup achieves maximum torque because the torque produced by the motor is directly proportional to the

current on the q-axis, while the flux of the d-axis rotor remains constant. With this feature, electromagnetic torque is used not only for driving the motor but also for implementing brake functions to minimize torque ripple during commutation. The above parameters can be implemented into the system through automatic settings in the VESC software interface, as shown in Figure 7.

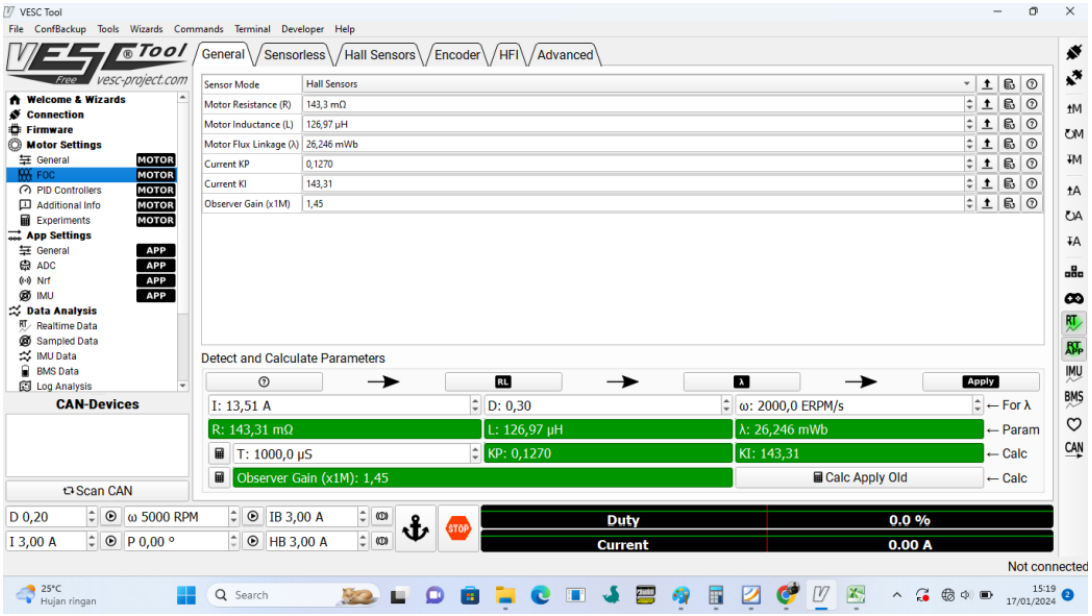

Figure 7: FOC Setting for BLDC Setup

3.3 Braking Control Mechanism

Plug braking, also known as counter-current braking, is an effective electric braking method for BLDC motors. This technique involves altering the phase sequence of the input current to dissipate braking energy within the motor itself. Unlike rheostatic and regenerative braking, plug braking requires an external energy source to supply the braking force. However, it provides a sufficiently strong braking force to be used in emergency situations, unlike the other two methods.

The principle of plug braking involves reversing the direction of the magnetic field by altering the phase sequence of the three-phase current. This method is applied to the BLDC model, which is utilized for high-performance control and is detailed in Section 2. The BLDC model is analyzed in various reference frames, including the framework d–q for control purposes.

The eight switching states of SVPWM are transferred to the motor driver design to switch from V_7 (111) $\rightarrow$ V_6 (101) $\rightarrow$ V_5 (100) $\rightarrow$ V_4 (110) $\rightarrow$ V_3 (010) $\rightarrow$ V_2 (011) $\rightarrow$ V_1 (001) $\rightarrow$ V_0 (000) with voltage combinations 0, $-Vs$ and V_s assigned to V_{uv}, V_{vw} and V_{wu}. It is possible to control the rotation of the motor by setting the frame of reference to a certain quantity of the motor.

Traditional regenerative brakes can easily be realized here for the purpose of recharging the battery. This can be accomplished by disconnecting the drive unit and inverter and directing the back-EMF through the inverter to the battery as shown in Figure 4, but with the SVPWM switching state reversed. Note that because the IGBT does not have a body diode, diodes must be added to the collector and emitter to correct the sinusoidal stator waveform.

Furthermore, following the previous design [10], the function of the electromagnetic brake system is also built in to keep the vehicle's slip ratio within the ideal range of the safety brake, namely ABS, by adjusting the duty cycle of the driving current flow.

The braking process uses the electromotive force generated by the BLDC due to the inertial force on the vehicle without a controller which will impact the driver because the vehicle stops suddenly and causes discomfort. Based on these facts, the author added the braking mechanism using the variable duty cycle in Pulse-width modulation (PWM).

4 Implementation

To verify the performance of the regenerative braking system, hardware implementation is required in the form of an electric bicycle unit using a BLDC motor. As shown in Figure 8, the frame is specially designed to support the regenerative braking system. This frame was selected based on the criteria for rigid materials to ensure that safety and riding comfort are maintained.

Figure 8: The Experimental Setup

Figure 9: The integrated driving/braking converter uses Flipsky 75/100

The converter circuit is shown in Figure 9. This converter can be used as a driver to drive the BLDC hub and can also be used as a battery charger when braking. In this study the battery system used is 72 Volt or 20S lithium. To improve optimization in this converter, the use of a MOSFET with a high current rating and low R_{ds} is used as an option, in addition to dead-time being also added to prevent cross-conduction when driving or braking.To validate this regenerative braking system, direct road testing is required. Figure 10 shows the route used for this testing.

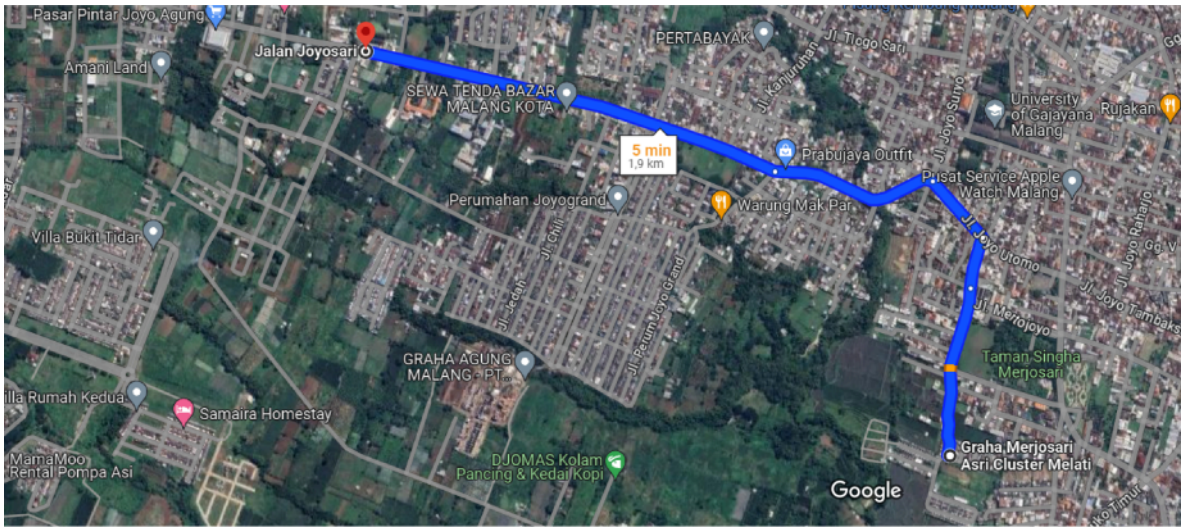

Figure 10: Road Testing Route Map

5 Result and Discussion

Figure 11 illustrates the regenerative current observed during testing. The drive region represents the current during acceleration, while the regenerative region displays the reverse current during braking. The presence of a negative current in the regenerative region confirms that a reverse current is generated during deceleration. This reverse current is stored back in the battery, allowing the electric vehicle to achieve a longer range compared to a system without regenerative braking.

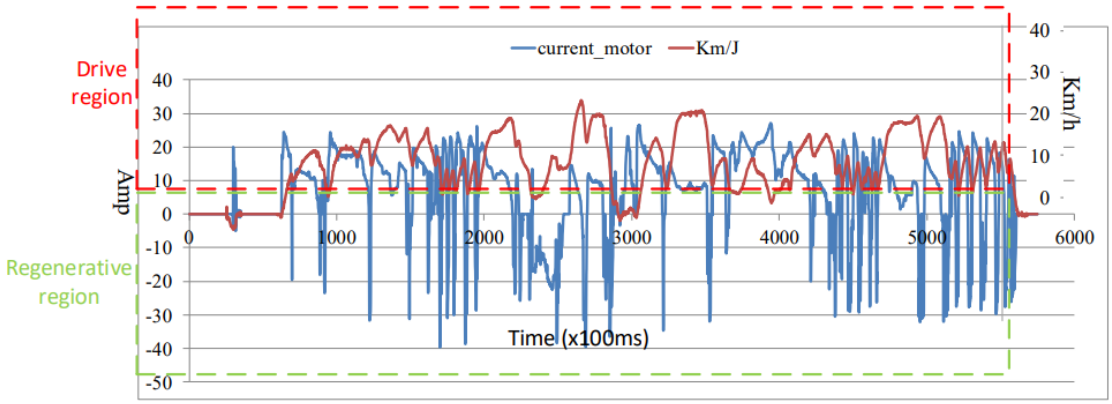

Figure 11: Data results driving/braking

Figure 12 displays the energy generated during braking, expressed in ampere-hours (Ah). For a detailed breakdown of the exact amount of energy generated from the braking process, refer to Table 1.

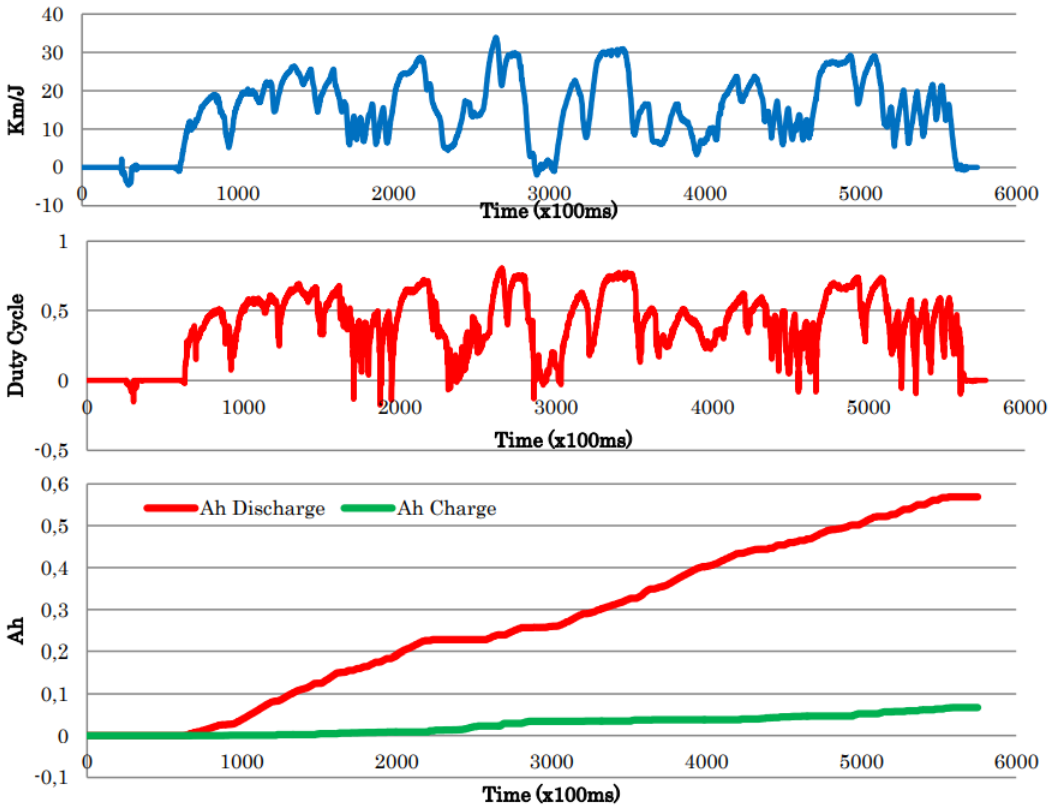

Figure 12: Speed, Duty Cycle, and Ah Graphs During Testing

Table 1. Comparison of Initial Condition versus Final COndition of Braking Test

Parameter	Initial Condition	Final Condition
Battery Voltage(V)	53,7 Volt	52,9 Volt
Ah Draw (mAh)	0 mAh	569 mAh
Ah Charge (mAh)	0 mAh	67,1 mAh
Wh Draw (Wh)	0 Wh	30,1 Wh
Wh Charge (Wh)	0 Wh	3,5 Wh
Distance (Meter)	0 Km	3,8 Km
Time	0	10 minute (600000 ms)

In this study, data collection was performed by recording data in real-time as the electric vehicle was driven on the road. From the tests, it was found that the total energy recovered during braking was 3.5 W_h, while the energy required to drive was 30.1 W_h. Based on this, it can be concluded that the energy recovered from the brake was 11.7% of the energy consumed during acceleration.

6 Conclusion

Most electric vehicles currently employ conventional braking systems, such as brake pads that attach to the wheel disks. However, this traditional method is not ideal for electric vehicles due to its inefficiency. Instead, regenerative braking systems are commonly used, which convert the energy lost during braking into electrical energy to recharge the battery. In this study, we integrated a regenerative braking system with

other electric braking systems, using a new variable obtained by pulling the brake lever. The aim was to improve both both safety and comfort of the driver of an electric motorcycle. We implemented a regenerative brake system that utilizes the Field-Oriented Control (FOC) algorithm. The FOC system offers benefits such as minimal ripple, low noise, and high efficiency compared to other methods. Additionally, the reverse-FOC braking scheme provides a satisfactory response at both high and low speeds. These advantages contribute to improved control during electric vehicle operation and greater energy savings. The energy recovered from braking was 11.7% of the energy consumed during acceleration. The experiment was conducted on a road with real-time data logging to measure the energy recovered from the braking process, using a modified 250-watt BLDC motor.

Acknowledgement

This research is fully supported and funded by DIPA-Polinema.

References

[1] G. Tzortzis, A. Amargianos, S. Piperidis, E. Koutroulis, and N. C. Tsourveloudis, "Development of a compact regenerative braking system for electric vehicles," in *2015 23rd Mediterranean Conference on Control and Automation (MED)*. IEEE, June 2015.

[2] R. E. Hellmund, "Regenerative braking of electric vehicles," *Transactions of the American Institute of Electrical Engineers*, vol. 36, pp. 1–78, January 1917.

[3] M. Gupta, "Evaluation of regenerative braking and its functionality in electric vehicles," in *2020 International Conference for Emerging Technology (INCET)*. IEEE, June 2020.

[4] F. Genduso, R. Miceli, C. Rando, and G. R. Galluzzo, "Back emf sensorless-control algorithm for high-dynamic performance pmsm," *IEEE Transactions on Industrial Electronics*, vol. 57, no. 6, pp. 2092–2100, June 2010.

[5] O. C. Kivanc and O. Ustun, "Investigation of regenerative braking performance of brushless direct current machine drive system," *Applied Sciences*, vol. 11, no. 3, p. 1029, February 2021.

[6] J. Jiang and J. Holtz, "An efficient braking method for controlled ac drives with a diode rectifier front end," *IEEE Transactions on Industry Applications*, vol. 37, no. 5, pp. 1299–1307, 2001.

[7] K. T. Chau and Y. S. Wong, "Overview of power management in hybrid electric vehicles," *Energy Conversion and Management*, vol. 43, no. 15, pp. 1953–1968, 2002.

[8] T.-D. Ton, M.-F. Hsieh, and P.-H. Chen, "A novel robust sensorless technique for field-oriented control drive of permanent magnet synchronous motor," *IEEE Access*, vol. 9, pp. 100 882–100 894, 2021.

[9] M. Aktas, K. Awaili, M. Ehsani, and A. Arisoy, "Direct torque control versus indirect field-oriented control of induction motors for electric vehicle applications," *Engineering Science and Technology, an International Journal*, vol. 23, no. 5, pp. 1134–1143, 2020. [Online]. Available: https://www.sciencedirect.com/science/article/pii/S2215098619326734

[10] F. Yusivar, N. Hidayat, R. Gunawan, and A. Halim, "Implementation of field oriented control for permanent magnet synchronous motor," in *2014 International Conference on Electrical Engineering and Computer Science (ICEECS)*. IEEE, November 2014.

[11] A. Saghafinia, H. Ping, and M. Uddin, "Sensored field oriented control of a robust induction motor drive using a novel boundary layer fuzzy controller," *Sensors*, vol. 13, no. 12, pp. 17 025–17 056, December 2013.

[12] S.-M. Liu, C.-H. Tu, C.-L. Lin, and V.-T. Liu, "Field-oriented driving/braking control for electric vehicles," *Electronics*, vol. 9, no. 9, p. 1484, September 2020.

[13] A. Al Shaheer, S. M. Hammad, and F. I. Bakhsh, "Analysis of speed and torque of a BLDC motor through field-oriented control using SVPWM scheme," in *Proceedings of the International Conference on Sustainable Power and Energy Research*. Singapore: Springer Nature Singapore, Feb. 2024, pp. 167–183.

[14] M. Karabacak, D. Hrvanovic, E. Ipek, E. B. Ivanoski, N. Köster, H. Haberl, and G. Prochart, "Accurate BLDC modeling and interleaved control for multi-motor powertrains with improved FOC to mitigate battery current and torque ripples," *IEEE Access*, vol. 13, pp. 209 328–209 355, Dec. 2025.

[15] M. M. Elkholy, M. M. Algendy, and E. A. El-Hay, "Modern control techniques and operational challenges in permanent magnet synchronous motors: A comprehensive review," *Automation*, vol. 6, no. 4, p. 49, Sep. 2025.

[16] N. Prabhu, R. Thirumalaivasan, and B. Ashok, "Critical review on torque ripple sources and mitigation control strategies of BLDC motors in electric vehicle applications," *IEEE Access*, vol. 11, pp. 115 699–115 739, Oct. 2023.

[17] A. K. Junejo, W. Xu, and Y. Tang, *Advanced Sliding Mode Control for Electric Machines and Drive Systems*. Boca Raton, FL, USA: CRC Press, Feb. 2026.

[18] Z. Zhu, S. Wang, B. Shao, L. Yan, P. Xu, and Y. Ren, "Advances in dual-three-phase permanent magnet synchronous machines and control techniques," *Energies*, vol. 14, no. 22, p. 7508, Nov. 2021.

[19] A. Kumar, M. V. Naik, R. Kumar, and Aman, "Design and analysis of BLDC motor speed control for electric vehicles powered by solar PV and grid supply," *Discover Electronics*, vol. 2, no. 1, p. 60, Jul. 2025.

[20] R. S. Pillai, M. Kalbande, and D. M. Deshpande, "Field oriented control of PV-BESS fed traction PMSM drive for EV application," in *Proceedings of the International Conference on Emerging Trends in Sustainable Systems (ICETS 2024)*. Singapore: Springer, 2024, pp. 121–131.

[21] W. Chen, "Comparison of doubly-fed induction generator and brushless doubly-fed reluctance generator for wind energy applications," Ph.D. dissertation, Newcastle University, Newcastle upon Tyne, UK, 2014.

[22] P. Peng, "Design and control of a brushless doubly-fed machine for aviation propulsion," Ph.D. dissertation, The Ohio State University, Columbus, OH, USA, 2020.

[23] L. Harnefors, "Design and analysis of general rotor-flux-oriented vector control systems," *IEEE Transactions on Industrial Electronics*, vol. 48, no. 2, pp. 383–390, Aug. 2002.

[24] A. Flah, I. A. Khan, A. Agarwal, L. Sbita, and M. G. Simoes, "Field-oriented control strategy for double-stator single-rotor and double-rotor single-stator permanent magnet machine: Design and operation," *Computers & Electrical Engineering*, vol. 90, p. 106953, Mar. 2021.

[25] H. Sun, T. Zhang, and J. Jiang, "Zero-vector-reconfiguration-based SVPWM technique for ZVZCS and voltage spike suppression in high-frequency-link three-phase AC–DC converter," *IEEE Transactions on Power Electronics*, vol. 39, no. 5, pp. 5536–5546, Feb. 2024.

[26] R. Pittini, "High efficiency reversible fuel cell power converter," Ph.D. thesis, Technical University of Denmark, Department of Electrical Engineering, Lyngby, Denmark, 2014.